Modelling solar radiation in forest canopy for the purposes of forest growth modelling

Marek Fabrika, Ján Merganič
Technical University Zvolen, Forestry faculty, Department of forest management and geodesy, T.G. Masaryka 24, 960 53 Zvolen, Slovakia, E-mail: fabrika@vsld.tuzvo.sk, merganic@vsld.tuzvo.sk

Introduction

Recently, empirical and semi-empirical models have been applied in forest modelling with great success. Their advantage is that they are coupled with empirical data of the population, for which they were constructed. Hence, they have good statistical characteristics, and they respect the requirements on model precision and accuracy. However, their disadvantage is caused by the lack of the answers on the questions about the processes, which take place in a forest ecosystem. At Technical University of Zvolen, a semi-empirical tree distance-dependent model named SIBYLA has been developed (FABRIKA 2005, FABRIKA and ĎURSKÝ 2006). The growth simulator consists of several basic components: structure generator (A), 3-D structure model (B), calculation model (C), mortality model (D), disturbance model (E) thinning model (F), competition model (G), growth model (H), and forest regeneration model (I). The core of the simulator (D, G, H) uses the modelling approach of the simulator SILVA 2.2 (PRETZSCH and KAHN 1998). The models were modified following the calibration process. Model (A) comprises the parts which were taken over (generating horizontal coordinates of trees and their crown parameters), and those which were modified (generating tree diameters and heights). Model (C) was completely redesigned to ensure that it considers the algorithms applied in Slovakia including the field of mensuration, ecology, and economics. Model (B) was newly created on the base of the principles of virtual reality. Similarly, models (E) and (F) are models newly developed in Slovakia. Model (I) is still under the development. For a more detailed description of individual models see (FABRIKA 2005). The smallest cycle that can be modelled is 1 year. The model produces information about production, ecology, and economy, but it does not simulate processes in forest ecosystems, such as photosynthesis, transpiration, allocation, etc. Due to this shortage our attempt has been to amend the model for modelling the physiological processes of trees in the form of down-scaling the simulations. The goal is to down-scale the empirical annual output about trees on a level of their organs and on shorter time periods (month, day, hour). The output will provide a user with the information about gross and net primary production (GPP, NPP), assimilation amount from photosynthesis, biomass allocation in tree organs, amount of transpired water, water use efficiency (WUE), carbon and nitrogen use efficiency (CUE, NUE), etc. The first step is to simulate the amount of solar radiation that is needed for modelling of photosynthesis and transpiration. The aim of the paper is to present the methodology of solar radiation modelling in the environment of the growth simulator SIBYLA, which will lead to refining of growth simulations. The model of solar radiation has been being developed within the module called Astronomer, which derives the amount of direct and diffuse radiation that is absorbed in the crowns of individual trees.

Data

Different data sources were used for the model construction. The model of cloudiness was derived from the measurements of 78 weather stations (Zborník prác SHMÚ 1991) located at altitudes ranging from 100 to 2,635 m above sea level. The stations recorded the data about the relative average cloudiness in individual months of the year, as well as the number of clear days (up to 20% of cloudiness) and cloudy days (more than 80% of cloudiness) per month. The data cover 30-year measurements between 1951 and 1980. For modelling of hourly changes in cloudiness, the data from 4 local weather stations were used, which were situated in: Borová Hora (350 m n.m.), Boky Sever (510 m n.m.), Kráľová (785 m n.m.) and Predná Poľana (1264 m n.m.). These weather stations recorded the amount of solar radiation every 10 minutes. The hourly change of solar radiation was used to derive the hourly changes in cloudiness. The model was validated on the data from regular hourly measurements of changes in cloudiness at an airport Sliač for the period of one whole year. The visible horizon was modelled using the digital terrain model of Slovakia in grid of 90 x 90 m.

Model methodology

The model of radiation consists of the model of radiation at open space and the model of radiation in a forest canopy. The model of radiation at open space is composed of the model of cloudiness, the model of horizon, the model of sun's position, and the model of the radiation amount at open space. The model of radiation in a forest canopy consists of the model of radiation absorption in the upper hemisphere of the crown, and the model of radiation absorption in the crowns of individual trees.

Model of cloudiness

The model simulating the number of clear days (with cloudiness less than 20%) was derived from the data from 78 weather stations. This model is a function of the month and the altitude:

$$Cleardays = a_0 + a_1.Altitude + a_2.Month + a_3.\ Altitude^2 + a_4.\ Altitude.\ Month + a_5.\ Month^2 \quad (1)$$

Similarly, the model of simulating the number of cloudy days (with cloudiness exceeding 80%) was developed:

$$Cloudydays = b_0 + b_1 . Altitude + b_2 . Month + b_3 . Altitude^2 + b_4 . Altitude . Month + b_5 . Month^2 \quad (2)$$

Table 1 and Figure 1 present the coefficients of the models and their performance, respectively.

Tab. 1: Coefficients of the models simulating the number of clear days (cloudiness below 20%) and cloudy days (cloudiness above 80%).

Model of clear days (cloudiness below 20%)					
a_0	a_1	a_2	a_3	a_4	a_5
2,218	-0,0022	0,8728	$7{,}2878.10^{-7}$	$6{,}6197.10^{-6}$	-0,0648
Model of cloudy days (cloudiness above 80%)					
b_0	b_1	b_2	b_3	b_4	b_5
19,3611	0,0049	-4,4057	$-1{,}2422.10^{-6}$	$-7{,}5751.10^{-5}$	0,3447

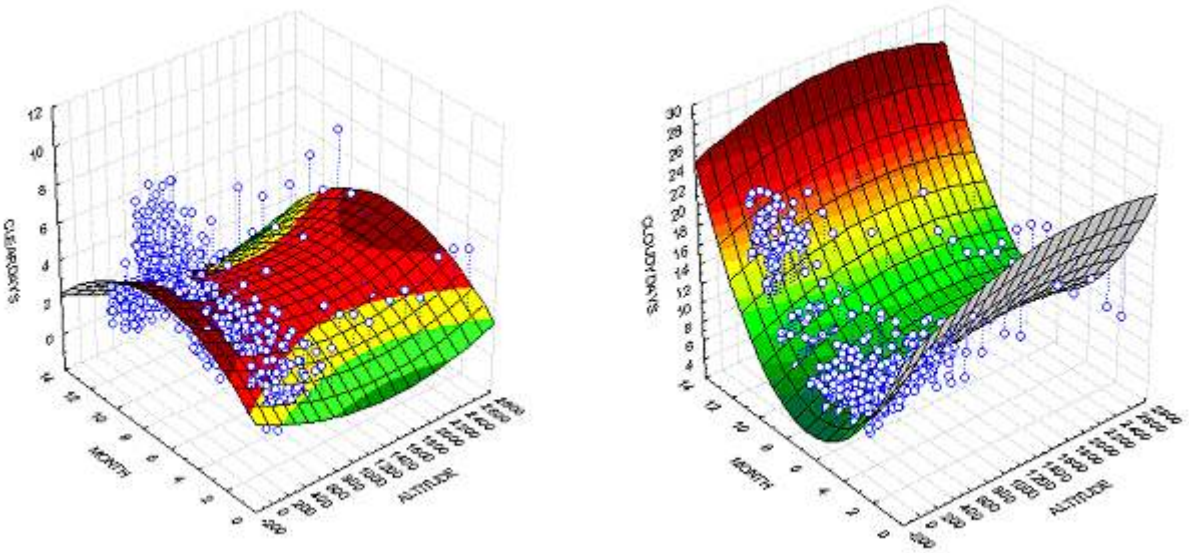

Figure 1: Model of the number of clear days (cloudiness below 20%) and cloudy days (cloudiness above 80%).

By subtracting the sum of the number of clear and cloudy days from the number of days in a particular month (monthdays), the number of the days with moderate cloudiness (from 20 to 80%) is calculated:

$$Moderatedays = Montdays - (Cleardays + Cloudydays) \quad (3)$$

On the base of the number of clear, cloudy and moderate days, the frequency distribution function of the cloudiness is generated (Figure 2). The function f(cloudiness) describes the number of hours with a particular cloudiness percentage (cloudiness) per month:

$$f(x) = c_0 + c_1 . cloudiness + c_2 . cloudiness^2 \quad (4)$$

The coefficients of the equation (c_0, c_1, c_2) were derived by solving the set of equations to ensure that the total numbers of clear, cloudy, and moderate days (cloudiness below 20%, above 80%, between 20 and 80%, respectively) were equal to the numbers from the models (1), (2) a (3).

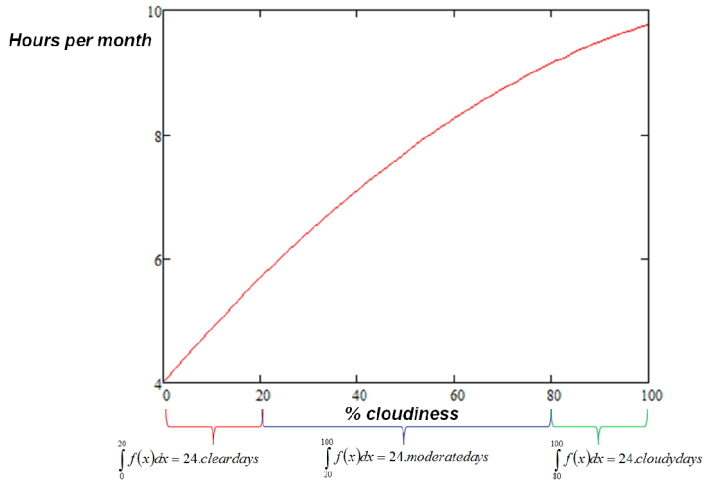

Figure 2: Frequency distribution function of cloudiness described as a number of hours per month

From the data recorded at local weather stations (Borová Hora, Boky Sever, Kráľová, Predná Poľana), hourly changes of cloudiness were derived on the base of the change of solar radiation using the index method with regard to the daily modelled performance of radiation in the case of no cloudiness. The model was validated using the data of cloudiness assessment with the precision of 1/8 at an airport Sliač. In case the cloudiness in the next hour increases by more than 1/8, it refers to cloudiness increase (S) in the model. If the modelled cloudiness decreases by more than 1/8, we talk about cloudiness decrease in the model (K). If the change of cloudiness falls inside the range ±1/8, it refers to steady cloudiness (R). The results of the model are the frequencies of cloudiness increases and decreases on the base of the calendar month (Month) according to the formula:

$$f(Month) = a + b.Month + c.\sqrt{x}.\ln(Month) \quad (5)$$

The values of the coefficients of the model describing cloudiness increase (S) are a= 0.28458, b= -0.09363, c= 0.11925, while for cloudiness decrease (K) the coefficients are a= 0.27307, b= -0.13703, c= 0.17575. The models are shown in Figure 3. The frequency of the days with unchanged cloudiness (R) is calculated as:

$$R = 1 - (S + K) \quad (6)$$

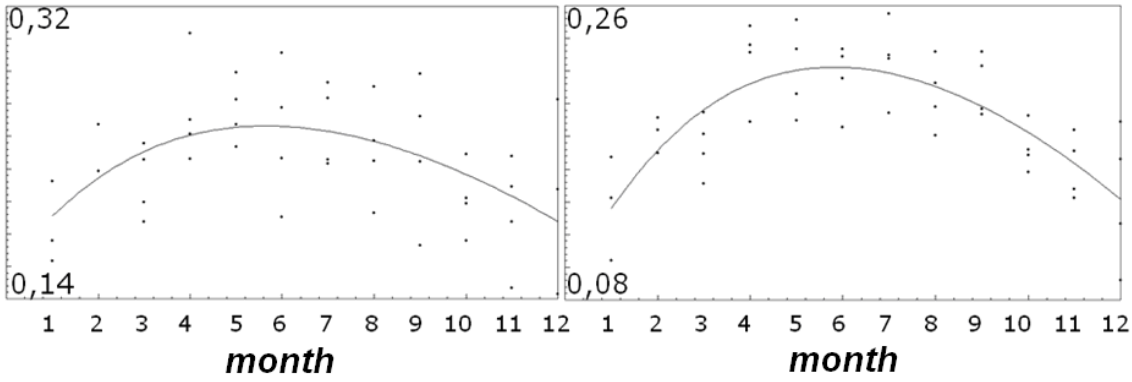

Figure 3: Frequency models of cloudiness increase or decrease in individual calendar months.

Hourly cloudiness in a particular month is then generated in a following way:

1. The starting value of cloudiness percentage is generated from the continuous frequency distribution function of cloudiness (Function 4).
2. The type of cloudiness change is generated from the discrete probability distribution of categories (S, K, R).
3. A new value of cloudiness percentage in the next hour is generated from the frequency distribution function of cloudiness (Function 4) until the generated value meets the condition of hourly change generated in step 2.
4. Steps 2 and 3 are repeated until the whole time sequence of cloudiness percentage in all hours per calendar month is generated.

Model of horizon

Using the digital terrain model of Slovakia in grid of 90 x 90 m, the horizon angles (i.e. angles of sky obstruction, FU and RICH 1999) in the direction from the centre of the pixel towards 4 cardinal and 4 ordinal directions (North, East, South, West, Northeast, Southeast, Southwest, Northwest) were calculated in ArcGIS environment. The analysis results in 8 raster layers (each layer for one direction), in which every pixel (90 x 90 m) represents the angle of horizon shading. On the base of the coordinates of a selected forest stand, the particular pixel is selected and the horizon angles are taken for all eight directions. The continuous model of horizon for each azimuth is then derived using cubic splines. An example presented in the hemispherical projection is given in Figure 4.

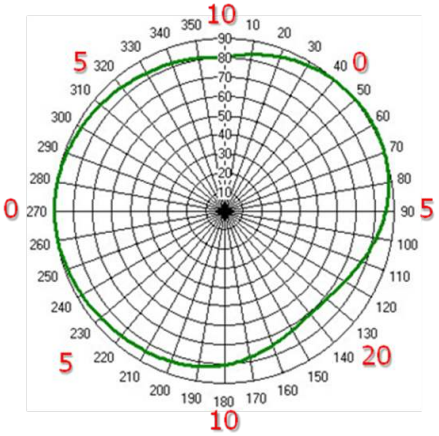

Figure 4: The principle of modelling visible horizon on the base of the model of horizon obstruction in eight directions, and the cubic spline interpolation (figure is presented in the hemispherical projection with a common assignment of directions, i.e. 0=North, etc.).

Model of sun's position

Sun's position in the sky, and hence, the incoming solar radiation at open space, is calculated using astronomical formulae (ASTRONOMICAL ALMANAC ONLINE 2008). The input variables in the model are: longitude and latitude of the forest stand, altitude, aspect, and slope. With regard to the specific day of year and time of day, the model calculates the following parameters of the sun's travel: right ascension, declination, inclination, geographical angle, geographical azimuth, global azimuth, angle height, solar noon, sunrise, sunset, length of solar day and solar night, average solar anomaly, relative distance of the sun in astronomical units (AU), and an absolute distance of the sun in kilometres. Figure 5 presents an example of outputs for May 17th 2010 at 2:00 pm. The output is valid for the forest stand situated at 500 m above seal level, with longitude -19.7° and latitude 48.8°. It has an eastern aspect and the slope of 15°. Figure 5 shows the travel of the Sun through the sky during the specific day, while the red point indicates its position in the given time of the day.

Model of radiation at open space

The amount of direct and diffuse radiation at open space is calculated depending on the sun's position, cloudiness, and obstructions in the horizon. First, the relative optical length (relopthlength) of radiation is calculated depending on altitude (altitude) and zenith angle of the sun (zenith) (RICH et al. 1994):

$$relopthlength = e^{\frac{-0{,}000118.altitude-1{,}638.10^{-9}.altitude^2}{\cos(zenith)}} \quad (7)$$

Secondly, the amount of direct solar radiation in a cloudless day (KREITH and KREIDER, 1978) (DIR_0) is calculated using solar constant (solarconst = 1367 W.m^{-2}), Linke atmospheric turbidity coefficient (LINKE 1922) (linke), solar constant of the relative distance of the sun in astronomical units (rsun), transmissivity of the atmosphere (transmissivity), relative optical length (relopthlength)′, and an angle of incidence of sun rays falling on the ground measured from the axis normal to the surface (inclination):

$$DIR_0 = linke.solarconst.rsun.transmisivity^{relopthlength}.\cos(inclination) \quad (8)$$

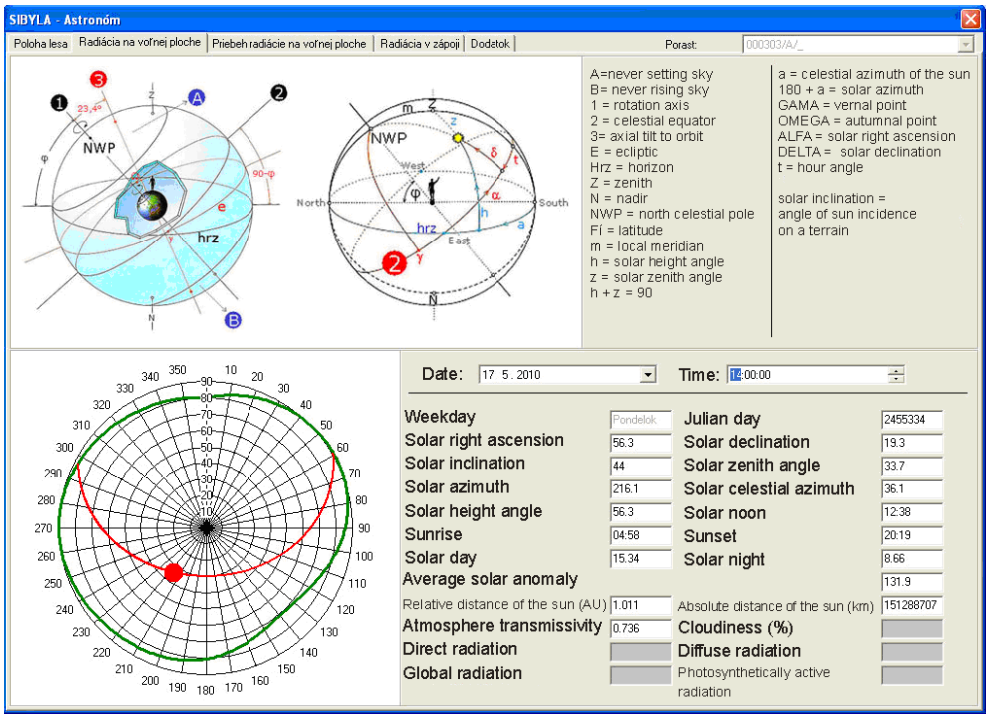

Figure 5: Output of the model of sun's position for the forest stand with geographical coordinates -19,7; 48,8; altitude 500 m a.s.l., East aspect, slope 15°, having the horizon as specified in Figure 4, on May 17th 2010 at 2:00pm.

Transmissivity of the atmosphere (KREITH and KREIDER, 1978) is dependent on the day of a year (day) and is calculated as follows:

$$transmisivity = 0{,}64 + 0{,}12.\cos\left(360.\frac{day - 174}{365}\right) \tag{9}$$

Diffuse radiation (DIF_0) is calculated similarly for a cloudless sky (KREITH and KREIDER, 1978), which is also dependent on the slope of the terrain (slope):

$$DIF_0 = 0{,}06.solarconst.rsun.transmisivity^{relopthlength}.\left(\frac{1 + \cos(slope)}{2}\right) \tag{10}$$

Global radiation at open space in a cloudless day is calculated as a sum of direct and diffuse solar radiation:

$$G_0 = DIR_0 + DIF_0 \tag{11}$$

The actual value of global radiation depends on the generated cloudiness (cloudiness):

$$G_C = cloudiness.G_0 \tag{12}$$

The actual values of diffuse (DIF) and direct radiation (DIR) are estimated from the formulae:

$$DIF_C = fraction.G_C \tag{13}$$

$$DIR_C = G_C - DIF_C \tag{14}$$

The fraction of diffuse radiation in equation (13) is derived with interpolation techniques (derived according to KREITH and KREIDER, 1978) depending on the cloudiness percentage according to the formula:

$$fraction = \frac{DIF_0}{G_0} + \left(0{,}7 - \frac{DIF_0}{G_0}\right).cloudiness \tag{15}$$

Model of the upper hemisphere of radiation interception

The radiation at open space is reduced to radiation that enters a forest stand (radiation interception). This model requires information about individual trees: tree species, coordinates within the plot, diameter, height, height to crown base, and the widest crown diameters. The upper hemisphere of the crown is simulated for every tree at three different points of the tree crown: crown top, the transition from the sunlit to the shaded part of the crown, and the crown base. The points are situated at the tree stem axis. Crown shapes are simulated with the algorithms from PRETZSCH (2001). The upper hemisphere is modelled using the hit-and-miss method. The principle is shown in Figure 6. In the cycle, a beam starts from the evaluated point at the tree. The length of the beam depends on the size of the simulated plot (a, b) according to the formula:

$$l = 1{,}2.\sqrt{\left(a^2 + b^2\right)} \tag{16}$$

The azimuth of the beam is changed iteratively with the step of 2° from the range 0° to 360°. The same step is used for the zenith of the beam from the range 0° to 90°. The number of obstructions is evaluated at every 0.20 m segment along the whole length of the beam. If the beam passes through a tree stem or terrain, it is regarded as an impenetrable obstruction (indicated as a star in Figure 6). These points are characteristic by 0% of transmitted radiation. As the beam passes through tree crowns of neighbouring trees, the number of cross-sectional points of the end of each 0.20 m segment with the crowns is counted in the particular direction, while tree species are accounted for in the evaluation separately. The number of cross-sectional points is then converted to the length of the barrier in meters: barrier = number of points x 0.20. The size of the barrier influences the percentage of the transmitted radiation according to Lambert-Beer law (MONSI and SAEKI 1953), which was modified with regard to model purposes as follows:

$$\%R = 100.e^{-\left(1-\frac{transparency}{100}\right).barrier.\sqrt{\left(LAD.\cos(zenith)\right)^2+\left(\frac{1}{LAD}.\sin(zenith)\right)^2}} \tag{17}$$

The other independent variable is the transparency of tree branches (transparency) in % (derived from ELLENBERG 1963) calculated as a weighted average of tree species, while the weights of tree species are estimated from the ratio of the lengths of the barriers of individual tree species (Table 2). In addition the calculation also accounts for the average leaf angle distribution (LAD, leaf angle distribution), which is tree species dependent (Table 2, derived from ROSS 1981). If the value is equal to 1, it refers to spherical leaf distribution. If the value is smaller than 1, the leaves are distributed vertically, while the value above 1 indicates horizontal distribution of leaves. Similarly to transparency, this characteristic is also calculated as a weighted average depending on tree species composition. An example of the output from the model of crown transparency is presented in Figure 7.

Table 2: Transparency of tree branches (transparency) and leaf area distribution (LAD) derived from ELLENBERG 1963 and ROSS 1981, respectively.

Tree species	Spruce	Fir	Pine	Beech	Oak
transparency	68	55	85	61	65
LAD	1,08	1,15	0,98	1	1

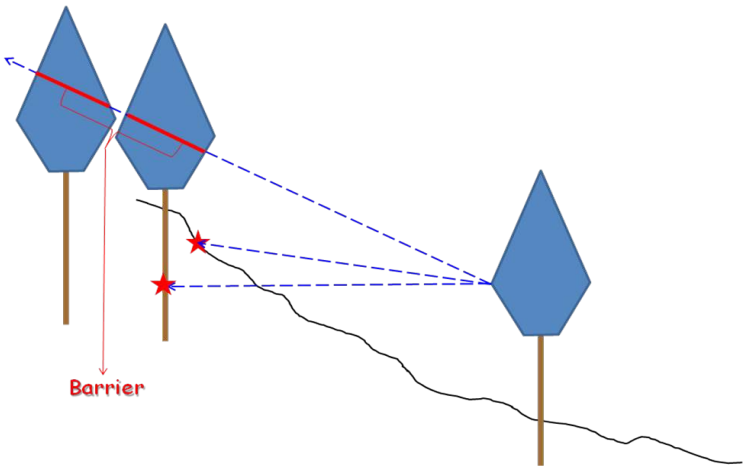

Figure 6: Hit-and-miss method applied in the simulation of the radiation interception in the upper hemisphere of the crown.

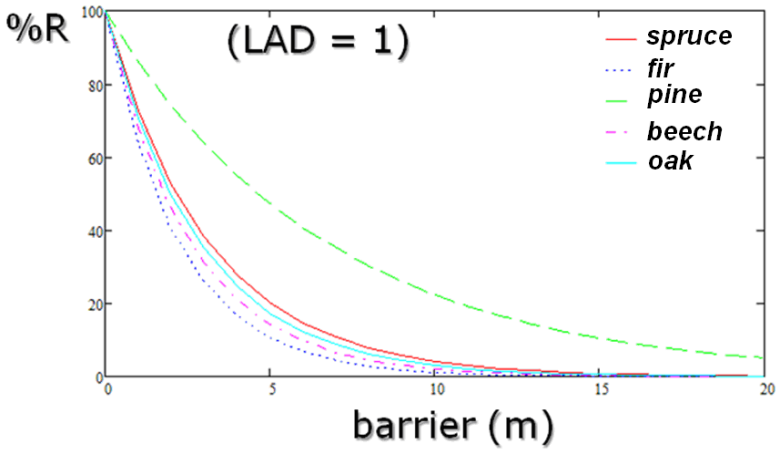

Figure 7: Model of crown transparency as a function of the length of the barrier separately for individual tree species and leaf area distribution LAD = 1.

In this way, the hemisphere is assessed at three points of stem axis. Figure 8 presents an example of the hemispheres for two selected trees: an understorey beech and a dominant spruce situated at one of the simulation plots of the simulator SIBYLA.

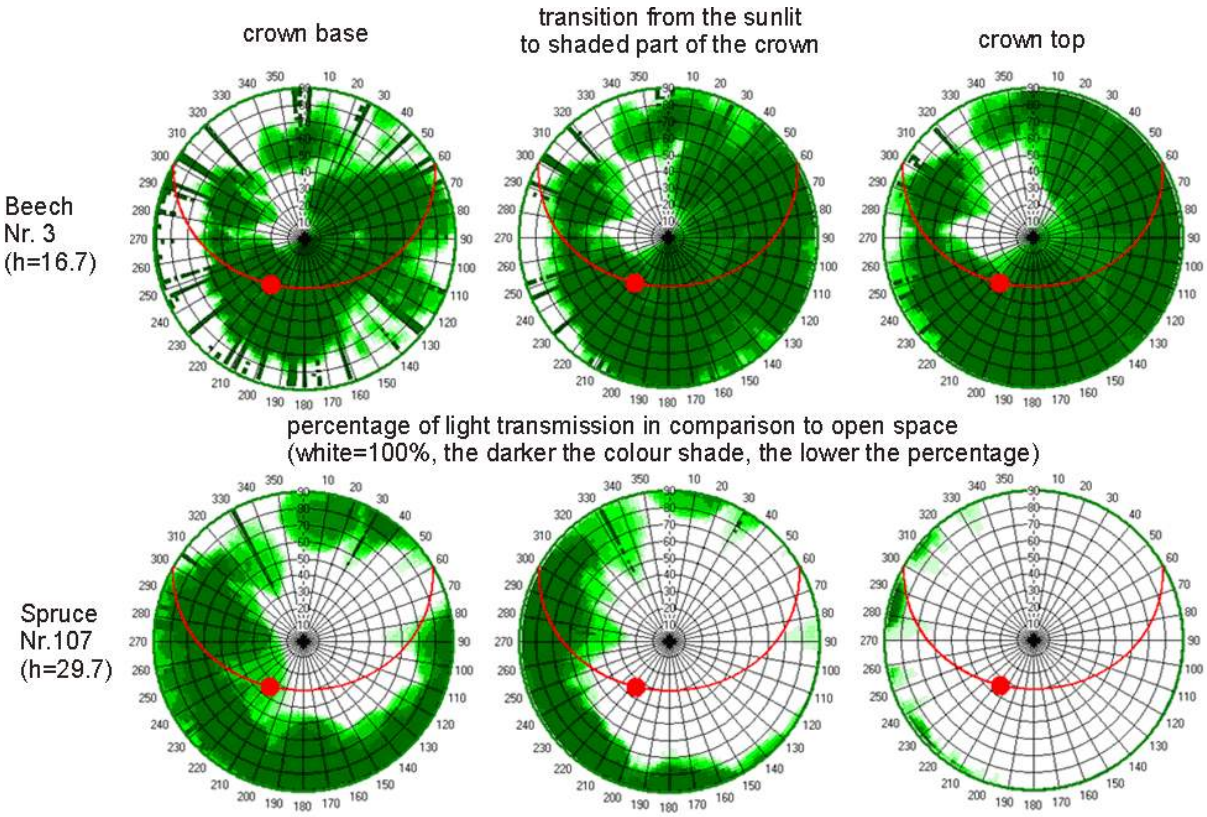

Figure 8: Example of hemispheres for two trees: an understorey beech and a dominant spruce. Hemispheres represent the tree top, the transition from the sunlit to shaded part of the crown, and the crown base.

Model of radiation absorption in crowns of individual trees

The model of the radiation interception in the upper hemisphere is used as a basis for the calculation of the percentage of direct and diffuse radiation. The percentage of the direct radiation is estimated as an arithmetical mean of the transmitted percentages of radiation in 10 sectors of the hemispheres, which are situated in the surrounding of the sun's position on the sky. Each sector represents a part of the sky of the size 2° of azimuth and 2° of zenith. The percentage of diffuse radiation is calculated as an arithmetical mean of all sectors of the hemisphere. In this way, the percentages of radiation are calculated for the top tree, the transition between the sunlit and the shaded part of the crown, and the crown base. The remaining points on the crown are interpolated as it is shown for the dominant spruce tree in Figure 9. This is the way how the amount of solar radiation absorbed by

leaves can be estimated in any height of the tree crown by reducing direct (DIR_C) and diffuse (DIF_C) radiation at open space by the percentage of the radiation transmitted through the stand canopy.

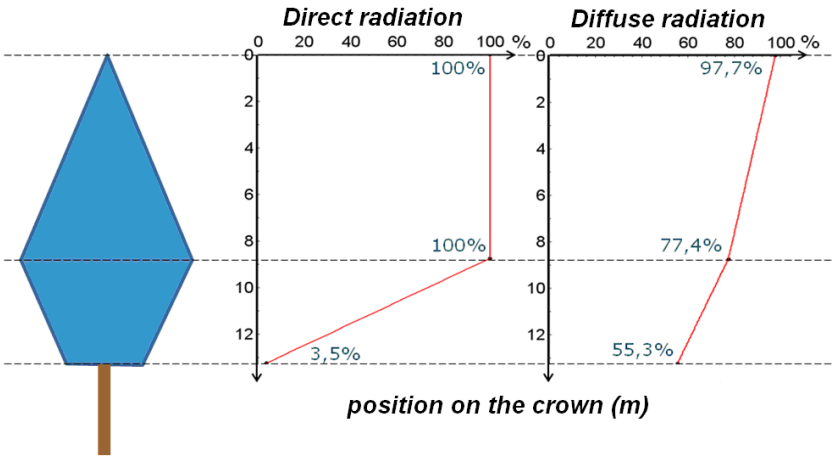

Figure 9: Radiation absorption along the crown of the spruce tree (No. 107) presented in Figure 8.

Conclusion

The presented model of solar radiation will enable us to refine the growth simulations of the tree semi-empirical model. The resulting simulations will down-scale the output at the level of tree organs and at a time period of 1 month, 1 day, or 1 hour. At the same time, they will also provide a user with the information about the ongoing processes, such as photosynthesis, transpiration, allocation, etc. The advantage of the model is that apart from the specification of the geographical position it does not require any other additional information to perform the simulation, since all other inputs represent standard components of growth simulations. Within the scope of our future research, it is required that the model is to be evaluated on the data describing the solar radiation in a forest canopy. Another so far unsolved question is the representativeness of the simulation plot of size 50 x 50 m, which, particularly in old loose stands, can cause that the model of the hemisphere does not account for the trees outside the plot that cause a decrease of solar radiation intensity, too. In this case, the appropriate solution seems to be to implement the correction model for the edge effect. A similar situation occurs if the assessed tree is situated at or near the boundary of the simulation plot. In such cases, the upper hemisphere is incomplete. The simplest solution would be to draw the boundaries of the simulation plot in the hemisphere, and to calculate the average value of diffuse radiation only from those sectors of the hemisphere that occur inside the simulation plot. If the sun's position lies in the sectors outside the simulation plot, we suggest reflecting its position into the quadrant of the hemisphere, which is completely filled with the forest simulation plot. The presented model of solar radiation represents a convenient amendment that refines growth simulations, which moves the simulations from the empirical towards the process-based approach.

Acknowledgment

This contribution/publication is the result of the project implementation: Centre of Excellence „Adaptive Forest Ecosystems", ITMS: 26220120006, supported by the Research & Development Operational Programme funded by the ERDF.

References

Astronomical Almanac Online, 2008: U.S. Nautical Almanac Office and Her Majesty's Nautical Almanac Office.

Ellenberg, H., 1963: Vegetation Mitteleuropas mit den Alpen: in kausaler, dynamischer und historischer Sicht. Verlag Eugen Ulmer, Stuttgart, 943 p.

Fabrika, M., 2005: Simulátor biodynamiky lesa SIBYLA, koncepcia, konštrukcia a programové riešenie. Habilitačná práca, Technická univerzita vo Zvolene, 238 p.

Fabrika, M., Ďurský, J., 2006: Implementing Tree Growth Models in Slovakia, In: Hasenauer, H., et al.: Sustainable Forest Management. Growth Models for Europe. Springer Berlin Heidelberg New York, 398 s, p. 315-341.

Fu, P, Rich, P.M., 1999: Design and Implementation of the Solar Analyst: an ArcView Extension for Modeling Solar Radiation at Landscape Scales. Accessed online 15. May 2010: http://proceedings.esri.com/library/userconf/proc99/proceed/papers/pap867/p867.htm

Kreith, F., Kreider, J. F., 1978: Principles of solar engineering. McGraw-Hill, New York, NY, 623 p.

Linke, F., 1922: Transmissions-Koeffizient und Trübungsfaktor. Beiträge zur Physik der freien Atmosphäre 10, p. 91-103.

Monsi, M, Saeki, T., 1953: Über den Lichtfaktor in den Pflanzengesellschaften und seine Bedeutung für die Stoffproduktion. Jap. J. Bot., 14, p. 22-52.

PRETZSCH, H., 2001: Modellierung des Waldwachstums. Parey Buchverlag Berlin, 341 p.

PRETZSCH, H., KAHN, M., 1998: Konzeption und Konstruktion des Wuchsmodells SILVA 2.2 - Methodische Grundlagen. Abschlußbericht Projekt W 28, Teil 2, München, 277 p.

RICH, P. M., DUBAYAH, R., HETRICK, W. A., SAVING, S. C., 1994: Using Viewshed models to calculate intercepted solar radiation: applications in ecology. American Society for Photogrammetry and Remote Sensing Technical Papers, p. 524-529.

ROSS, J., 1981: The radiation regime and architecture of plant stands, W. Junk, Boston, Massachusetts, 391 p.

ZBORNÍK PRÁC SLOVENSKÉHO HYDROMETEOROLOGICKÉHO ÚSTAVU, 1991: SHMÚ, Zväzok 33/I, Klimatické pomery Slovenska. Vybrané charaktersitiky, ALFA, Bratislava, 239 p.